COMPARISON OF UNMIXING RESULTS DERIVED FROM AVIRIS, HIGH AND LOW RESOLUTION, AND HYDICE IMAGES AT CUPRITE, NV

[1,2]Alexander F. H. Goetz and [1]Bruce Kindel

1.0 Introduction

The availability of low-altitude, high-spatial-resolution AVIRIS (Green et al, 1998) images and high-resolution HYDICE (Basedow et al, 1995) images over Cuprite, Nevada has provided an unprecedented opportunity to compare the radiometric quality, the ability to detect end-members and the application of matched filters to three different data sets in an area that is well-understood mineralogically. An earlier paper (Goetz and Kindel, 1996) compared high-altitude AVIRIS and HYDICE data and showed that, even though there was a 36:1 ratio in pixel area, no new end-members appeared in the HYDICE images that were not seen in the lower resolution AVIRIS data. This result was not surprising in light of the fact that the signal-to-noise ratio (SNR) of the HYDICE data was much lower than that of AVIRIS. In this study, it was possible to remove the uncertainty associated with differing SNR's because the same AVIRIS sensor was used to acquire both high-resolution and low-resolution images.

2.0 Image Data

The images used in this study were acquired by AVIRIS at 20 km altitude on June 18, 1998 and at 3.8 km altitude October 11, 1998. HYDICE images were acquired over Cuprite, Nevada on June 22, 1995. The only area common to all three sensors was a 2.3 km-long strip over the western portion of the eastern hydrothermal center covering the infamous "Buddingtonite Bump" and extending southward adjacent to "Kaolinite Hill" (fig 1).

3.0 Data Reduction and Analysis

3.1 Calibration

A subset of 50 bands in the 2.0-2.5 μm region was used from each data set. The assumption was made that the path radiance was negligible in this region. Each overflight included a pass over Stonewall Playa and the radiance values were normalized to reflectance using portable field reflectance measurements made of the Playa in December 1995 (Goetz and Kindel, 1996).

3.2 Image processing

Processing was undertaken using ENVI 3.1 software. Each data set was processed to produce a minimum noise fraction (MNF) image set. Figure 2 shows the AVIRIS MNF eigenvalues. The eigenvalues in both the high- and low-altitude data sets are quite similar, with a distinct dropoff after the eighth MNF band.

The fact that the first eigenvalue for the low-altitude data is greater may be associated with lower sun angle and greater area covered by shadows.

[1] Center for the Study of Earth from Space/CIRES
[2] Department of Geological Sciences, University of Colorado, Boulder 80309

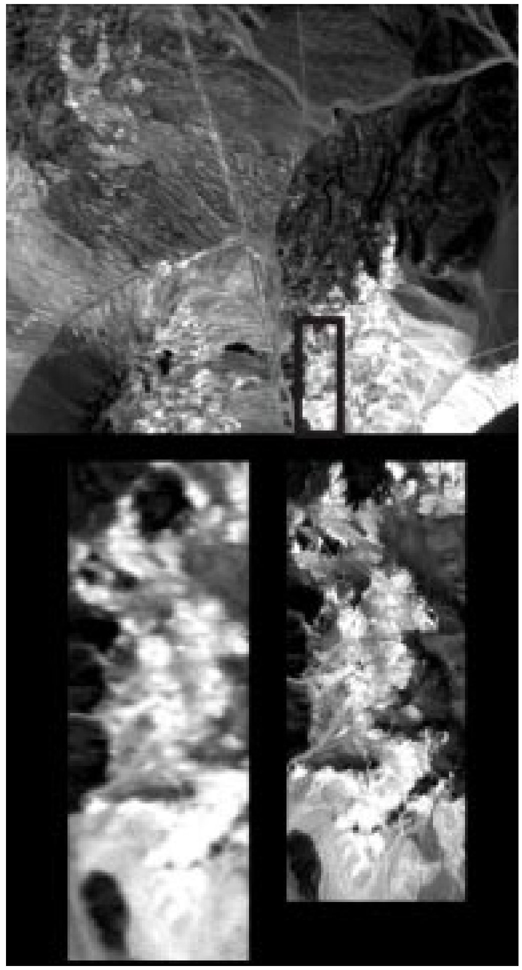

Figure 1. Top, full AVIRIS scene taken from 20 km altitude showing black box that outlines area covered by low-altitude overflight. Lower left, 8x8 resampled, high-altitude image to correspond with low-altitude image coverage. Lower right, low-altitude AVIRIS image at full resolution.

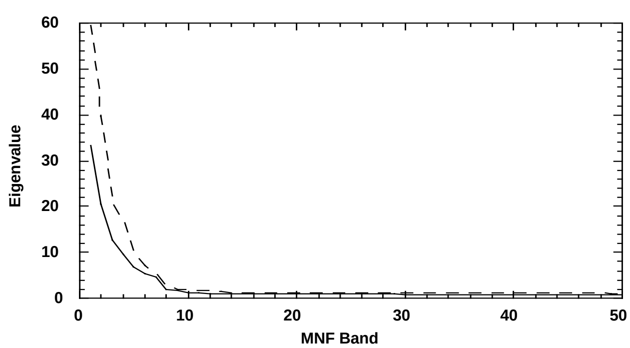

Figure 2. AVIRIS MNF eigenvalues. The dashed curve is for the low altitude data and solid curve is for the high altitude data.

The MNF images are shown in figure 3. In spite of the vastly different pixel sizes, the MNF images for the high-and low-altitude data sets are remarkably similar. Only in band 3 are there significant differences. On the other hand, the HYDICE MNF images are significantly different beyond the 5th MNF band because of all the sensor artifacts that masquerade as information.

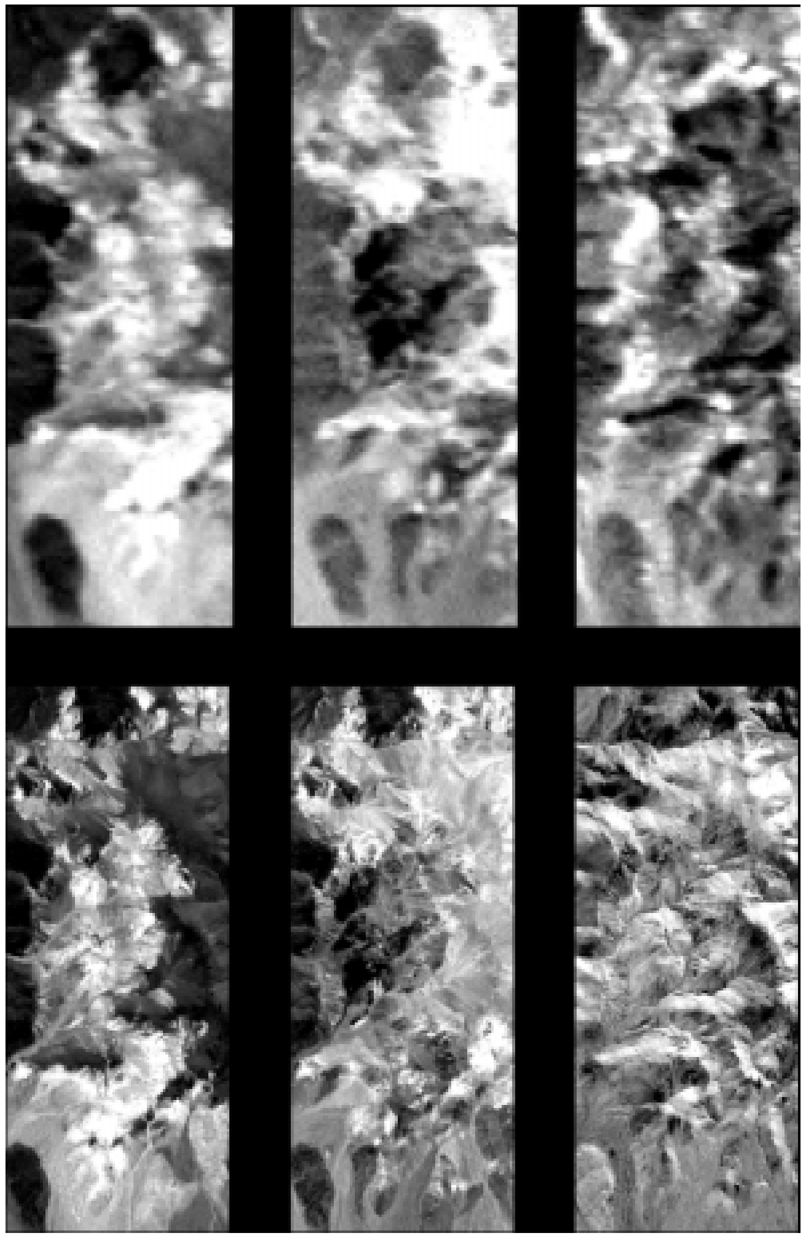

Figure 3. MNF images for bands 1-3. In each case, the upper image is from the high-altitude AVIRIS data.

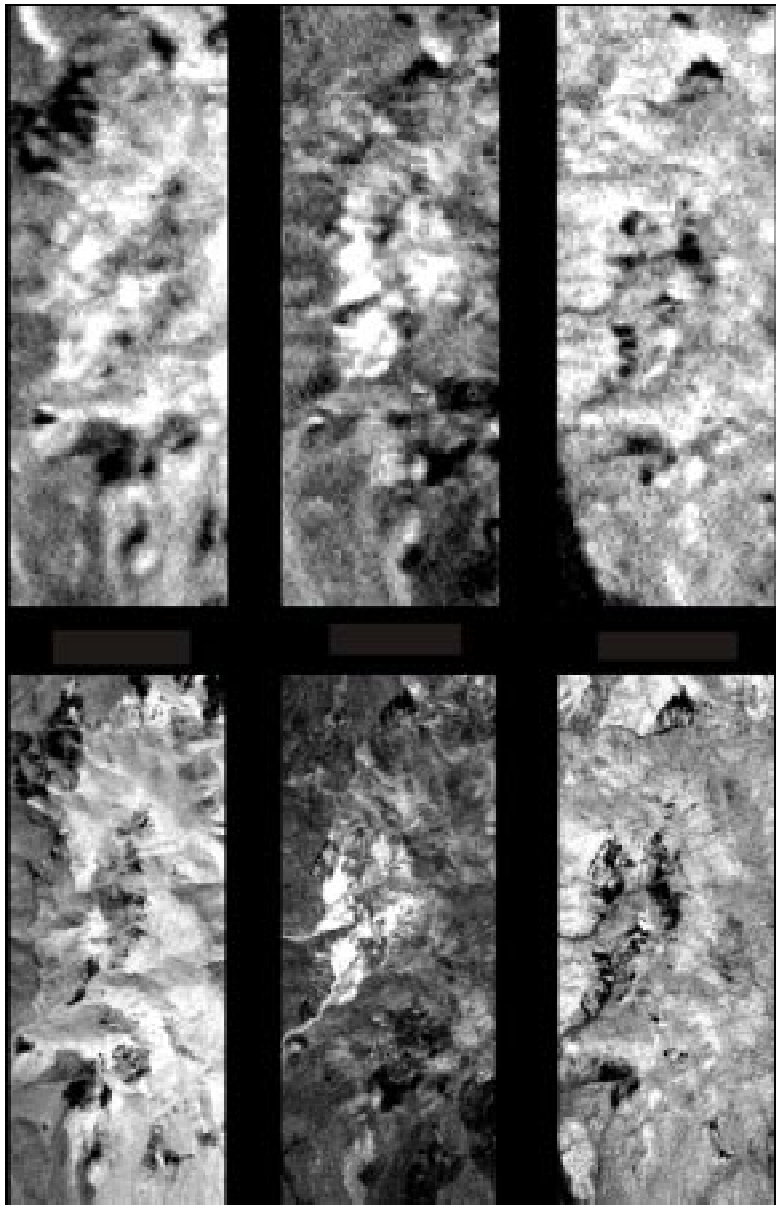

Figure 4. MNF images for bands 4-6. In each case, the upper image is from the high-altitude AVIRIS data.

3.3 Spectral analysis

A pixel-purity index analysis was run on both AVIRIS data sets in order to find the 300 purest pixels and from them identify the spectral end-members for thematic mapping. Figure 5 shows the 11 different spectral end-members identified by this process. The spectra are offset for clarity and correspond between data sets in sequence. Spectra of alunite, buddingtonite, (Felzer et al, 1994; Goetz and Srivastrava, 1985) kaolinite, dickite, and montmorillonite are easily recognizable. In general the low-altitude spectra have deeper absorption features, most likely associated with purer outcrops.

A series of matched filter images was constructed for buddingtonite, alunite, and kaolinite in order to compare the detectability for each in the different resolution images. The results for the first two minerals are shown in figures 6 and 7.

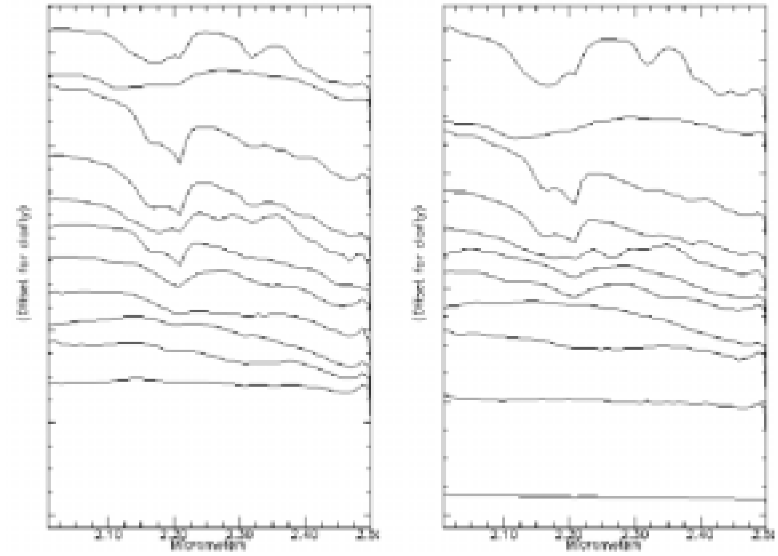

Figure 5. Spectra resulting from the pixel purity analysis for low-altitude data (left) and high-altitude data (right).

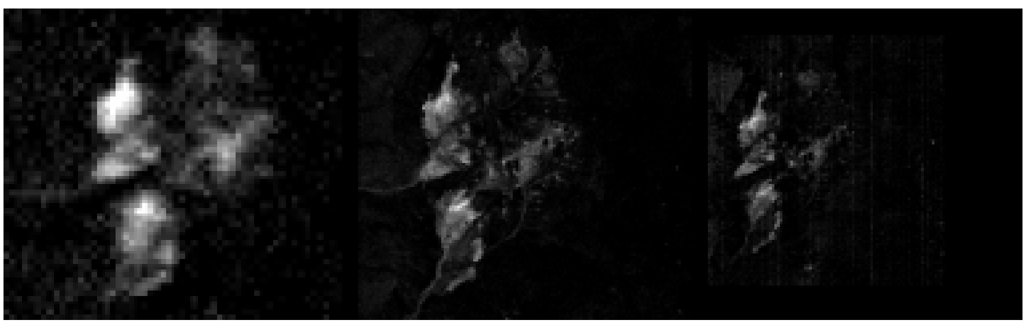

Figure 6. Matched filter, abundance images for buddingtonite as calculated from l-r, the high-altitude AVIRIS, low-altitude AVIRIS and HYDICE data. The HYDICE image is plotted at a smaller scale. The feature in the upper left corner is “Buddingtonite Bump”.

Figure 7 shows matched filter results for alunite in high-altitude and low-altitude AVIRIS. The results are unusual in that the center panel is the result of using the purest alunite spectrum in the high-resolution data, and it does not correspond with the alunite pixels presented in the left panel that is the low-resolution data. The right hand panel is again the high-resolution data matched filter presentation using an average of high-resolution spectra taken from the bright area shown in the bottom-right of the left panel. In this case, the bright areas in the left and right panel correspond.

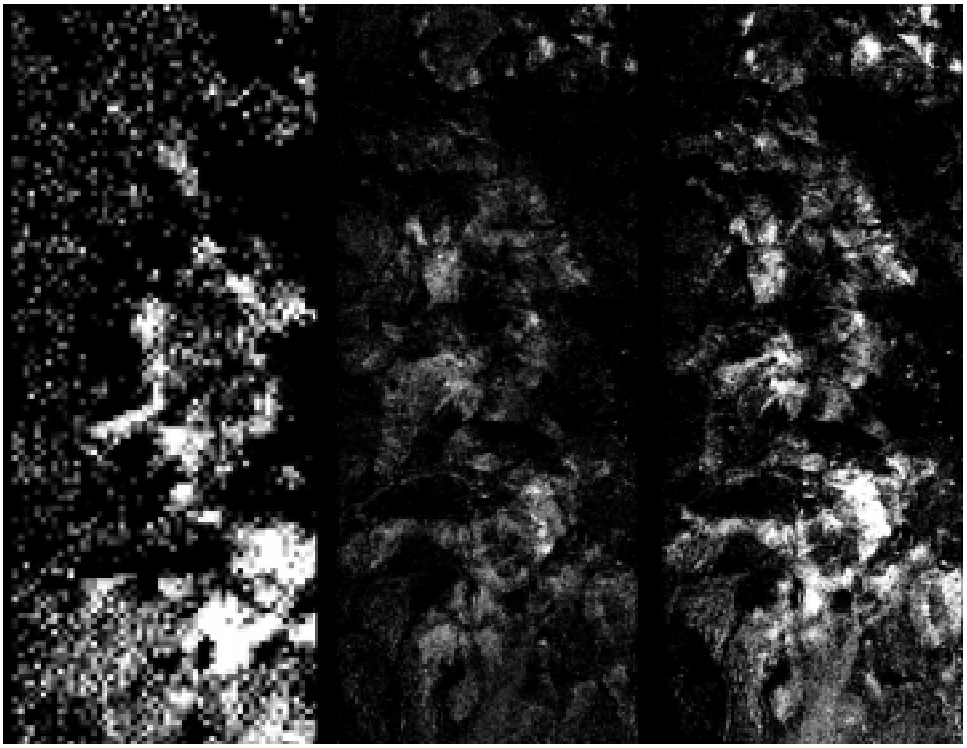

Figure 7. Matched filter images for alunite for, l-r, high-altitude, low altitude, low-altitude with averaged spectra.

Figure 8 shows the three spectra used for the matched filter calculations. The position of the spectral features is identical in each case, but the depth of the features is related to the purity. The sensitivity of the matched filter is in this case makes it difficult to compare the high- and low resolution results using spectra that, to the eye, appear to be from materials of identical composition. No doubt, the alunite spectra from the low-altitude data are from purer pixels. This intriguing result raises a flag of caution for users of matched filter algorithms. On the other hand, the results from buddingtonite in fig. 6 are quite comparable. The spectra in all three data sets are nearly identical. This, most likely, results from the fact that “Buddingtonite Bump” has been scraped off and presents a large uniform area that is well resolved in the high-altitude data.

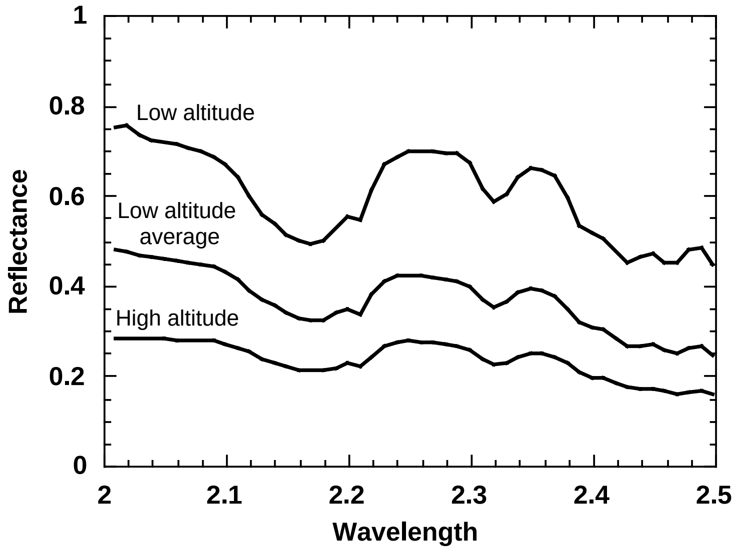

Figure 8. Alunite spectra used in creating the matched filter images in figure 7

3.4 Spatial analysis.

The dual-resolution data make it possible to investigate another parameter linked to the quality of unmixed data, namely signal-to-noise ratio (SNR). Low altitude image data were averaged to produce pixels the size of AVIRIS high-altitude pixels. The plot of eigenvalues is shown in figure 9. It shows the somewhat unexpected result that significant eigenvalues are obtained out to the 20^{th} MNF band indicating new endmembers not identified in the original high and low-altitude data, all of the same area.

Conventional wisdom dictates that an endmember, filling a portion of a pixel, will become less detectable as the pixels are averaged because its contribution to the total averaged spectrum will decrease. Increasing the SNR ratio will increase detectability approximately as the ratio of the area of the target material to the pixel area times the increase in SNR. However, the SNR increases only with the square root of the numbers of pixels averaged and, therefore, should not make targets more detectable.

The dilemma can be resolved by assuming that the endmembers are relatively uniformly distributed among all pixels. If so, an increase in SNR would result in the detection of materials making up a pixel, provided that all or most of the pixels contained the endmember material. The presence of new endmembers is seen in the scatter plots in figure 9. The center right plot shows a more compact, lower variance plot than the center-left plot of the low-altitude data. However the bottom panel shows that at MNF band 16 there are many more outlying points and, therefore, a greater variance in the averaged data than in the neat low-altitude data. Further study is required to identify these outliers.

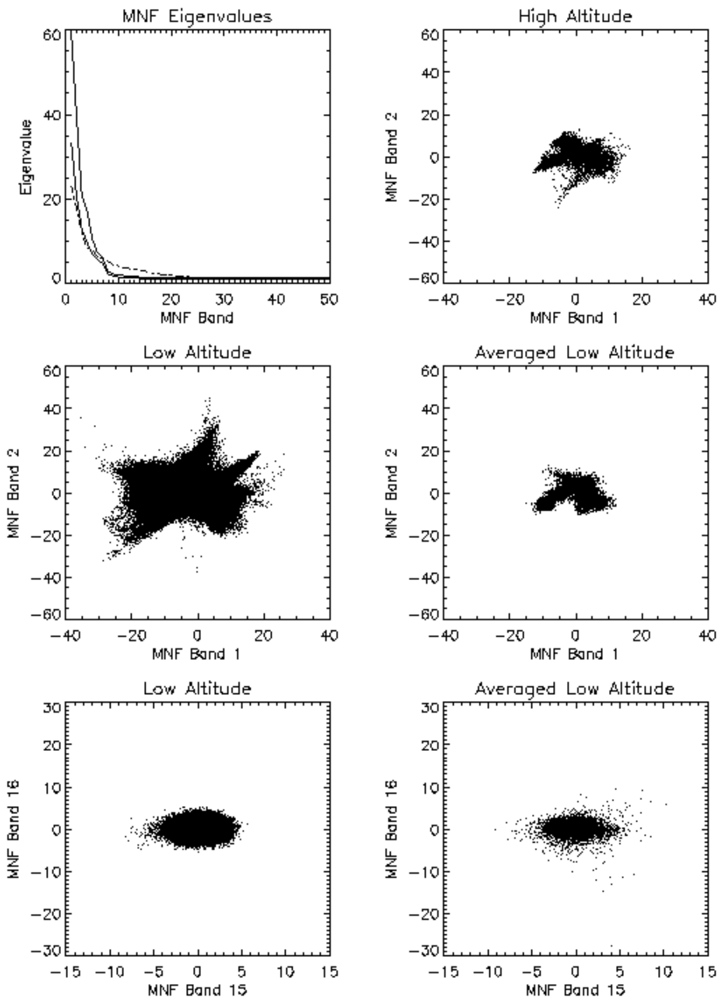

Figure 9. MNF Eigenvalues plot of high-altitude, low-altitude and low-altitude-averaged Cuprite data along with Scatter plots showing the increase in apparent unmixing end- member information in the low-altitude-averaged data.

4.0 Conclusions

The low-altitude, high resolution data over Cuprite, Nevada are of the highest quality and the 2.3 m pixel size makes it possible to identify mineral outcrops that are much less mixed with surrounding material than the 18 m pixels from the high altitude data. However, no new spectral endmembers were identified in the low-altitude data, only purer spectra of known mineral occurrences. It is possible that further, more detailed analysis of the low-altitude-averaged data will yield new mineral identifications or more subtle variations, such as ion substitutions, that were missed in this initial look at the data. At least in Cuprite, high-altitude AVIRIS images have sufficient resolution to identify and map all the major mineral occurrences. This result supports the conclusions reached in an earlier study (Goetz and Kindel, 1996) using HYDICE data with 3 m pixels but lower signal-to-noise ratios.

5.0 Acknowledgments

This research was supported under contract no. NAG5-4447 from the NASA Goddard Spaceflight Center. We appreciate the timely delivery of the low-altitude AVIRIS data, thanks to the Herculean efforts of the JPL AVIRIS team. We also wish to thank Joe Boardman of AIG for discussions and insight about the SNR effects.

6.0 References

Basedow, R. W., Armer, D. C. and Anderson, M. E., 1995, "HYDICE system: Implementation and performance," *Proceedings SPIE*, vol. 2480, pp.258-267.

Felzer, B., Hauff P., and A.F.H. Goetz, 1994 "Quantitative Reflectance Spectroscopy of Buddingtonite from the Cuprite Mining District, Nevada," *Journal of Geophysical Research-Solid Earth*, pp.2887-2895.

Goetz, A.F.H. and B. Kindel, 1996, "Understanding Unmixed AVIRIS Images in Cuprite, NV, using coincident HYDICE Data," *Summaries of the Sixth Annual JPL Airborne Earth Science Workshop*, Pasadena, California, pp. 96-103.

Goetz, A.F.H. and V. Srivastava, 1985 "Mineralogical Mapping in the Cuprite Mining District, Nevada," *Proceedings of the Airborne Imaging Spectrometer Data Analysis Workshop*, April 1985, *JPL Publication 85-41*.

Green, R.O. et al, 1998, "Imaging spectroscopy and the airborne visible/infrared imaging spectrometer (AVIRIS)," *Remote Sensing of Environment*, **65,** 227-248.